Numerical modeling of heat transfer and fluid flow in TIG arc welding with anode melting

Michel Brochard, Stephane Gounand, Marc Medale

Numerical modelling of heat transfer and fluid flow in TIG arc welding with anode melting

Michel Brochard

PHD Student,
CEA Saclay, DEN/DANS/DM2S/SEMT/LTA,
91191 Gif-Sur-Yvette Cedex, France

June 3, 2008

Outline

Outline

Outline

Outline

Outline

Study domain and objectives

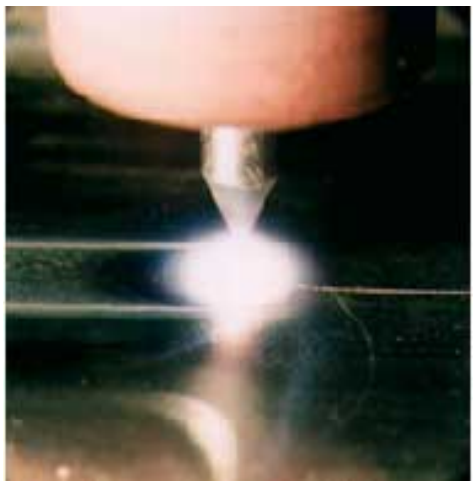

TIG process

Study domain

arc + anode (with weld pool) + cathode

Objectives

- Predict fluid flow and heat transfer in the arc plasma and in the weld pool
- Predict the weld pool shape in accordance with the workpiece proprerties
- Quantify the influence of each force acting in the weld pool on the weld pool shape, the arc drag force and the heat flux transferred to the workpiece

Study domain and objectives

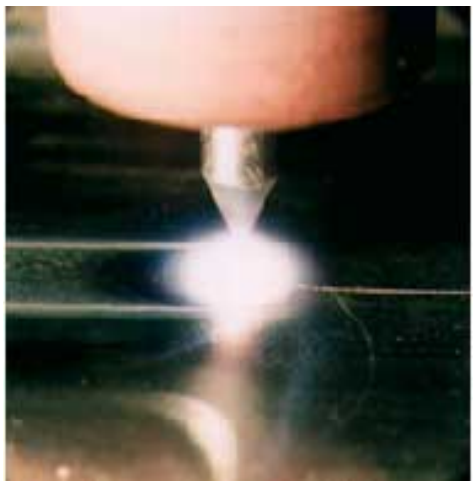

TIG process

Study domain

arc + anode (with weld pool) + cathode

Objectives

- Predict fluid flow and heat transfer in the arc plasma and in the weld pool
- Predict the weld pool shape in accordance with the workpiece proprerties
- Quantify the influence of each force acting in the weld pool on the weld pool shape, the arc drag force and the heat flux transferred to the workpiece

Outline

Physical phenomena involved

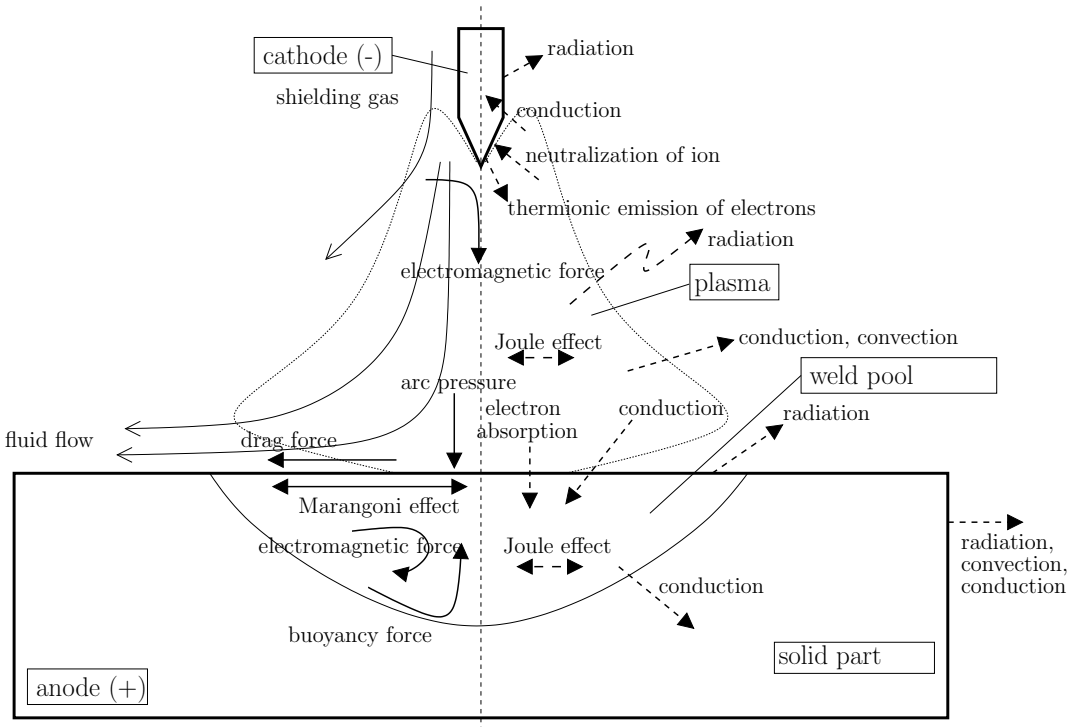

Physical phenomena involved in the process

Main contributions

- Joule heat (97% of total heat produced) [6]
- Lorentz force

↓

Need to implement an efficient electromagnetic model

Physical phenomena involved

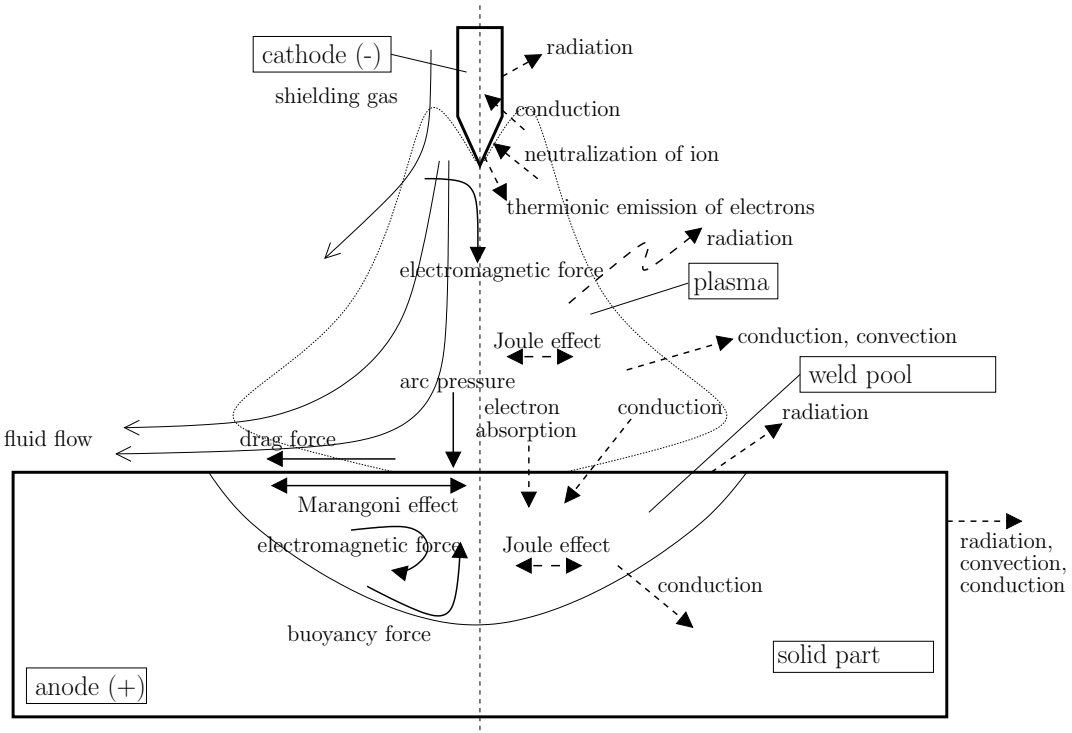

Physical phenomena involved in the process

Main contributions

- Joule heat (97% of total heat produced) [6]
- Lorentz force

↓

Need to implement an efficient electromagnetic model

Assumptions -1-

- Plasma is a fluid in Local Thermodynamic Equilibrium
- Magnetic convection is negligeable (small magnetic Reynolds number $R_{em} << 1$)
- Laminar (small Reynolds number $R_e < 2000$)
- Quasi-incompressibility (low Mach number : $M_a < 0.3$)
  $\Rightarrow$ Physical properties depend on the local temperature

$$R_{em} = V^* l^* \sigma^* {\mu_0}^* \approx 0.01 \quad R_e = \frac{\rho^* V^* l^*}{\mu^*} \approx 250$$
$$M_a = \sqrt{\frac{\rho^* V^{*2}}{\gamma^* P^*}} \approx 0.09$$

with : $V^* = 250\, m.s^{-1}$, $\gamma^* = 1.4$, $T^* = 15000\, K$, $\rho^* = 2.10^{-2}\, kg.m^{-3}$, $P^* = 101325\, Pa$, $\mu^* = 1.10^{-4}\, kg.m^{-1}.s^{-1}$, $l^* = 0.005\, m$, $\sigma^* = 8.10^3\, S.m^{-1}$, ${\mu_0}^* = 4\pi 10^{-7}\, H.m^{-1}$

Assumptions -2-

Gas and materials used

- Pure tungsten cathode
- Pure argon plasma at atmospheric pressure
- Anode in 304L steel

Geometry and system

- Two-dimensional axi-symmetric coordinates
- Material surfaces undeformable
- Steady state is assumed to exist

Assumptions -2-

Gas and materials used

- Pure tungsten cathode
- Pure argon plasma at atmospheric pressure
- Anode in 304L steel

Geometry and system

- Two-dimensional axi-symmetric coordinates
- Material surfaces undeformable
- Steady state is assumed to exist

Outline

For the plasma

Conservation equations

$$\text{Mass :} \quad \nabla \cdot (\rho \mathbf{u}) = 0$$

$$\text{Momentum :} \quad \rho \mathbf{u} \nabla \mathbf{u} + \nabla P - \nabla \cdot \bar{\bar{\tau}} = \mathbf{F}$$

$$\text{Energy :} \quad \rho C_p \mathbf{u} \cdot \nabla T - \nabla \cdot (\lambda \nabla T) = S$$

$$\text{with : } \bar{\bar{\tau}} = \mu \left[(\nabla \mathbf{u}) + (\nabla \mathbf{u})^T - \frac{2}{3} (\nabla \cdot \mathbf{u}) \bar{\bar{I}} \right]$$

Physical properties are taken from tables [1]

Source terms (with electromagnetic variables)

$$\mathbf{F} = \mathbf{F}_{Lorentz} + \mathbf{F}_{buoyancy} + \mathbf{F}_{resistance} = \mathbf{J} \times \mathbf{B} - \rho_{ref} \beta (T - T_{ref}) \mathbf{g} + K \mathbf{u}$$

$$S = S_{Joule} - S_{radiation} + S_{elec} = \frac{||\mathbf{J}||^2}{\sigma} - 4\pi \varepsilon_n$$

The net emission coefficient ε_n depends on the temperature [6]

For the plasma

Conservation equations

$$\text{Mass :} \quad \nabla \cdot (\rho \mathbf{u}) = 0$$

$$\text{Momentum :} \quad \rho \mathbf{u} \nabla \mathbf{u} + \nabla P - \nabla \cdot \bar{\bar{\tau}} = \mathbf{F}$$

$$\text{Energy :} \quad \rho C_p \mathbf{u} \cdot \nabla T - \nabla \cdot (\lambda \nabla T) = S$$

$$\text{with : } \bar{\bar{\tau}} = \mu \left[(\nabla \mathbf{u}) + (\nabla \mathbf{u})^T - \frac{2}{3} (\nabla \cdot \mathbf{u}) \bar{\bar{I}} \right]$$

Physical properties are taken from tables [1]

Source terms (with electromagnetic variables)

$$\mathbf{F} = \mathbf{F}_{Lorentz} + \mathbf{F}_{buoyancy} + \mathbf{F}_{resistance} = \mathbf{J} \times \mathbf{B} - \rho_{ref} \beta (T - T_{ref}) \mathbf{g} + K \mathbf{u}$$

$$S = S_{Joule} - S_{radiation} + S_{elec} = \frac{||\mathbf{J}||^2}{\sigma} - 4\pi \varepsilon_n$$

The net emission coefficient ε_n depends on the temperature [6]

For the weld pool (Boussinesq approximation)

Conservation equations

$$\begin{aligned}
\text{Mass :} \quad & \nabla \cdot (\rho \mathbf{u}) = 0 \\
\text{Momentum :} \quad & \rho \mathbf{u} \nabla \mathbf{u} + \nabla P - \nabla \cdot \bar{\bar{\tau}} = \mathbf{F} \\
\text{Energy :} \quad & \rho C_p \mathbf{u} \cdot \nabla T - \nabla \cdot (\lambda \nabla T) = S
\end{aligned}$$

with : $\bar{\bar{\tau}} = \mu \left[(\nabla \mathbf{u}) + (\nabla \mathbf{u})^T - \frac{2}{3} (\nabla \cdot \mathbf{u}) \bar{\bar{I}} \right]$

Physical properties are taken from tables [3]

Source terms (with electromagnetic variables)

$$\mathbf{F} = \mathbf{F}_{Lorentz} + \mathbf{F}_{buoyancy} + \mathbf{F}_{resistance} = \mathbf{J} \times \mathbf{B} - \rho_{ref} \beta (T - T_{ref}) \mathbf{g} + K \mathbf{u}$$

$$S = S_{Joule} - S_{radiation} + S_{elec} = \frac{\|\mathbf{J}\|^2}{\sigma} - 4\pi\varepsilon_n$$

The net emission coefficient ε_n depends on the temperature [6]

For the solid parts of electrodes

Conservation equations

$$\begin{aligned} \text{Mass :} \quad \nabla \cdot (\rho \mathbf{u}) &= 0 \\ \text{Momentum :} \quad \rho \mathbf{u} \nabla \mathbf{u} + \nabla P - \nabla \cdot \bar{\bar{\tau}} &= \mathbf{F} \\ \text{Energy :} \quad \rho C_p \mathbf{u} \cdot \nabla T - \nabla \cdot (\lambda \nabla T) &= S \end{aligned}$$

$$\text{with : } \bar{\bar{\tau}} = \mu \left[(\nabla \mathbf{u}) + (\nabla \mathbf{u})^T - \frac{2}{3} (\nabla \cdot \mathbf{u}) \bar{\bar{I}} \right]$$

Physical properties are taken from Metals Handbook

Source terms (with electromagnetic variables)

$$\mathbf{F} = \mathbf{F}_{Lorentz} + \mathbf{F}_{buoyancy} + \mathbf{F}_{resistance} = \mathbf{J} \times \mathbf{B} - \rho_{ref} \beta (T - T_{ref}) \mathbf{g} + K \mathbf{u}$$

$$S = S_{Joule} - S_{radiation} + S_{elec} = \frac{||\mathbf{J}||^2}{\sigma} - 4\pi \varepsilon_n$$

The net emission coefficient ε_n depends on the temperature [6]

Electromagnetic equations

Current density **J** calculation

Faraday's law :	$\nabla \times \mathbf{E}$	$=$	$\mathbf{0}$	$\Rightarrow \mathbf{E} = -\nabla\phi$
Ohm's law	$\mathbf{J}$	$=$	$\sigma\mathbf{E}$	$\Rightarrow \mathbf{J} = -\sigma\nabla\phi$
Charge conservation equation :	$\nabla \cdot \mathbf{J}$	$=$	0	$\Rightarrow \nabla \cdot (\sigma\nabla\phi) = 0$

Magnetic field **B** calculation

Ampere's law : $\nabla \times \mathbf{B} = \mu_0 \mathbf{J}$

Gauss's law : $\nabla \cdot \mathbf{B} = 0$

} first order system

$\rightarrow$ Lead to difficulties when solving by classical Galerkin method

Electromagnetic equations

Current density **J** calculation

Faraday's law :	$\nabla \times \mathbf{E}$	$=$	$\mathbf{0}$	$\Rightarrow \mathbf{E} = -\nabla\phi$
Ohm's law	$\mathbf{J}$	$=$	$\sigma\mathbf{E}$	$\Rightarrow \mathbf{J} = -\sigma\nabla\phi$
Charge conservation equation :	$\nabla \cdot \mathbf{J}$	$=$	0	$\Rightarrow \nabla \cdot (\sigma\nabla\phi) = 0$

Magnetic field **B** calculation

Ampere's law : $\nabla \times \mathbf{B} = \mu_0 \mathbf{J}$
Gauss's law : $\nabla \cdot \mathbf{B} = 0$
} first order system

$\rightarrow$ Lead to difficulties when solving by classical Galerkin method

Electromagnetic equations

Current density **J** calculation

Faraday's law :	$\nabla \times \mathbf{E}$	$=$	$\mathbf{0}$	$\Rightarrow \mathbf{E} = -\nabla\phi$
Ohm's law	$\mathbf{J}$	$=$	$\sigma\mathbf{E}$	$\Rightarrow \mathbf{J} = -\sigma\nabla\phi$
Charge conservation equation :	$\nabla \cdot \mathbf{J}$	$=$	0	$\Rightarrow \nabla \cdot (\sigma\nabla\phi) = 0$

Magnetic field **B** calculation

Ampere's law : $\nabla \times \mathbf{B} = \mu_0 \mathbf{J}$
Gauss's law : $\nabla \cdot \mathbf{B} = 0$
} first order system

$\longrightarrow$ Lead to difficulties when solving by classical Galerkin method

Outline

The Least Square Finite Element Method (LSFEM) [2]

Equation to solve

$$\int_\Omega (\nabla \times \mathbf{B}) \cdot (\nabla \times \mathbf{B}^*)\, d\Omega + \int_\Omega (\nabla \cdot \mathbf{B}) \cdot (\nabla \cdot \mathbf{B}^*)\, d\Omega = \int_\Omega \mu_0 \mathbf{J}_{imp} \cdot (\nabla \times \mathbf{B}^*)\, d\Omega$$

with $\mathbf{B}^*$ the weighting function of the trial function $\mathbf{B}$

Advantages

- Divergence of $\mathbf{B}$ is easily included
- Can be applied for 3D problems
- Give a symmetric, positive definite system that can be solved easily with iterative method

Outline

Additional energy terms [6]

On the cathode surface

$Q_a = q_{radiation} + q_{emission} + q_{ion} = -\sigma_B \epsilon T^4 - J_e \phi_c + J_i V_a$
where σ_B is the Stefan-Boltzmann constant, ϵ the cathode surface emissivity, T the temperature, ϕ_c the cathode work function, V_a the ionization potential of argon, J_i the ion current density, and J_e the electron current density.
$J_i = ||\mathbf{J}|| - J_r$ if $||\mathbf{J}|| - J_r > 0$, else $J_i = 0$
and $||\mathbf{J}|| = J_e + J_i$
$J_r = AT^2.exp\left(\frac{-e\phi_e}{k_b T}\right)$
where e is the elementary charge, k_b the Boltzmann's constant, A the thermionic emission constant , ϕ_e the effective cathode work function

On the anode surface

$Q_a = q_{radiation} + q_{absorption} = -\sigma_B \epsilon T^4 + ||\mathbf{J}||\phi_a$

where ϕ_a is the anode work function

Additional force term on the anode surface

Surface tension gradients :

$$\mathbf{F}_{\text{marangoni}} = \frac{\partial \gamma(T, a_i)}{\partial T} \frac{\partial T}{\partial \tau} \boldsymbol{\tau}$$

with a_i the activity of sulfur and $\boldsymbol{\tau}$ the tangential vector of the weld pool surface.

The surface tension γ from [5] :

$$\gamma(T, a_i) = \gamma_f - A(T - T_f) - RT\Gamma_s \ln\left[1 + k_1 a_i \exp\left(-\frac{\Delta H^0}{RT}\right)\right]$$

where γ_f is the surface tension of the pure metal at melting point, T_f is the melting point of the material, A is the negative of $\partial\gamma/\partial T$ for pure metal, Γ_s is the surface excess of saturation, k_1 is the entropy factor, and ΔH^0 is the standard enthalpy of adsorption. (Values are taken from [5])

Outline

Main boundary conditions and discretization

Discretization

- linear elements Q1 for the pressure and quadratic elements Q2 for the other variables
- Finite element code Cast3M
- LSFEM formulation used to compute **B**

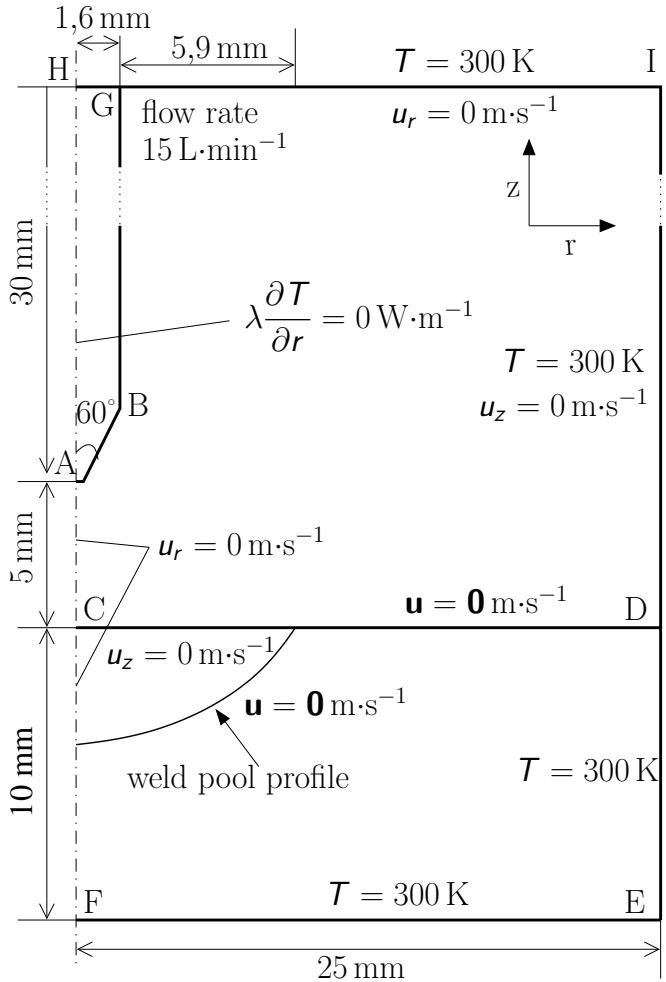

Geometry and boundary conditions

Outline

The arc part validation

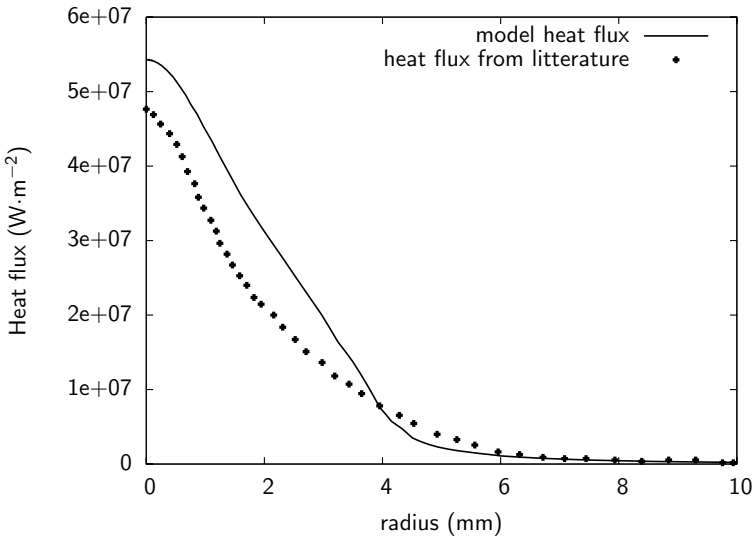

Comparison of calculated heat flux (W·m^{-2}) on the anode surface with litterature heat flux (Lowke [4]) for a 150 A arc with copper anode

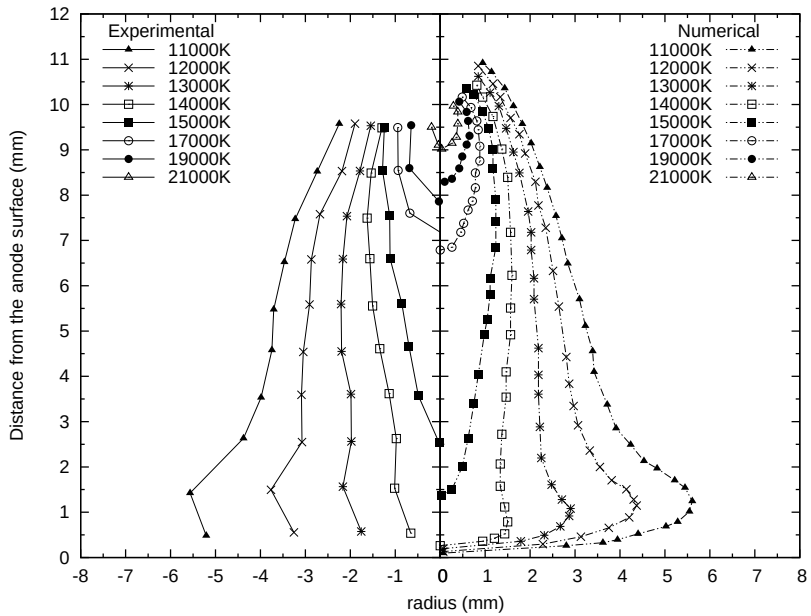

Comparison of temperatue profiles (K) with litterature experiment (Hsu [?]) for a 200 A arc with copper anode

→ Results in accordance with litterature model and experiments

Validation of the weld pool shapes

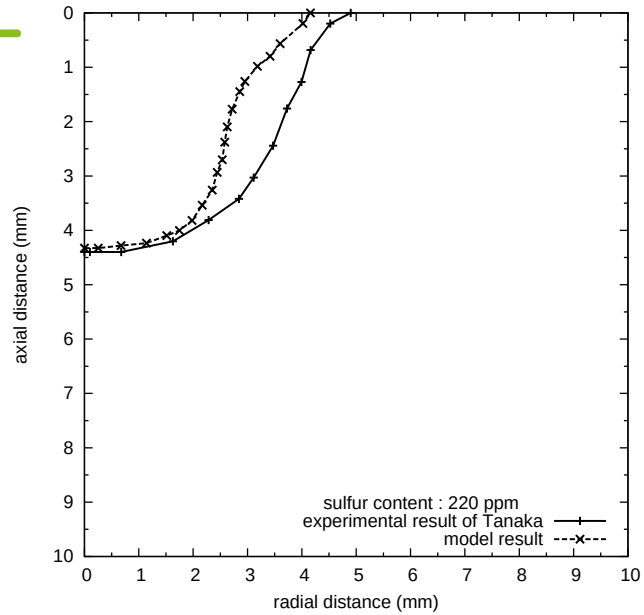

Comparison of weld pool profile (K) with litterature experiment (Tanaka and al. [6]) for a 150 A arc with 304L steel anode with 220 ppm of sulfur

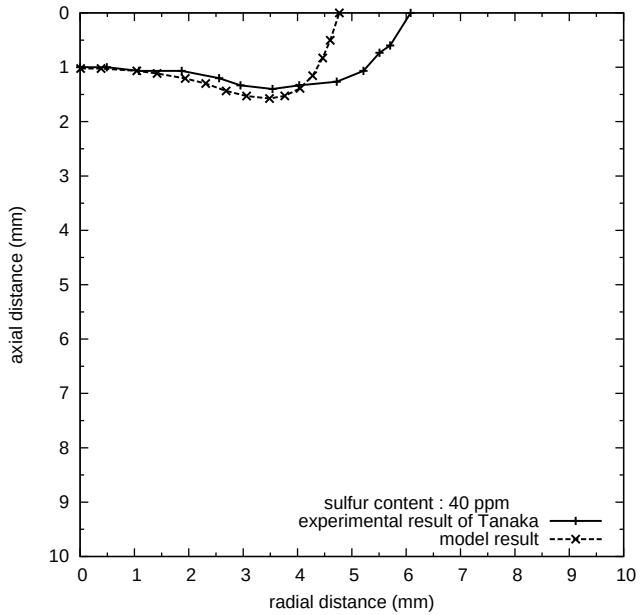

Comparison of weld pool profile (K) with litterature experiment (Tanaka and al. [6]) for a 150 A arc with 304L steel anode with 40 ppm of sulfur

- Results in accordance with litterature model and experiment
- The weld pool width is slightly underestimated : can be due to differences in the thermophysical propertie of the workpiece

Outline

Which forces are predominants ?

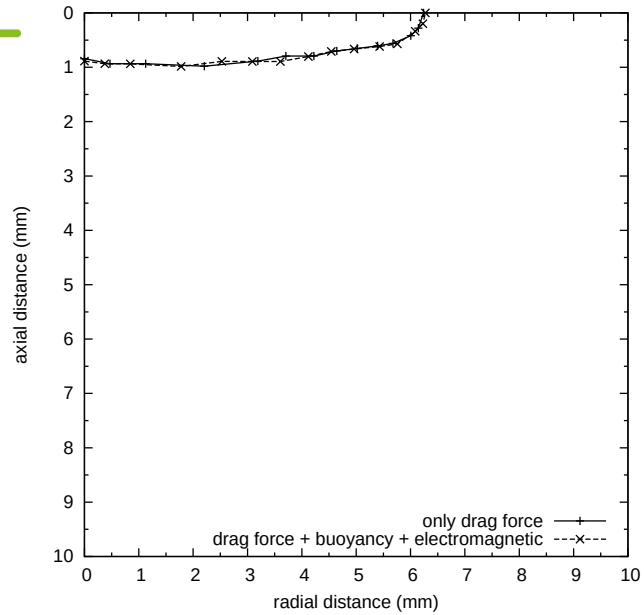

Influence of buoyancy, electromagnetic and arc drag forces on the weld pool shape

X

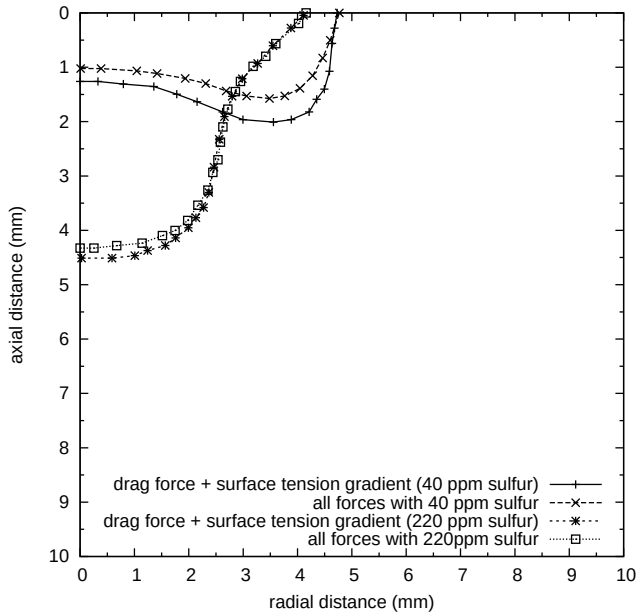

Influence of buoyancy, electromagnetic forces and surface tension gradient on the weld pool shape

- Drag and surface tension gradient forces are predominants
- The combinaison of buoyancy and electromagnetic forces tend to increase the weld depth
- Conclusions in accordance with litterature results

What is the influence of the weld pool shapes on the weld pool boundary conditions ?

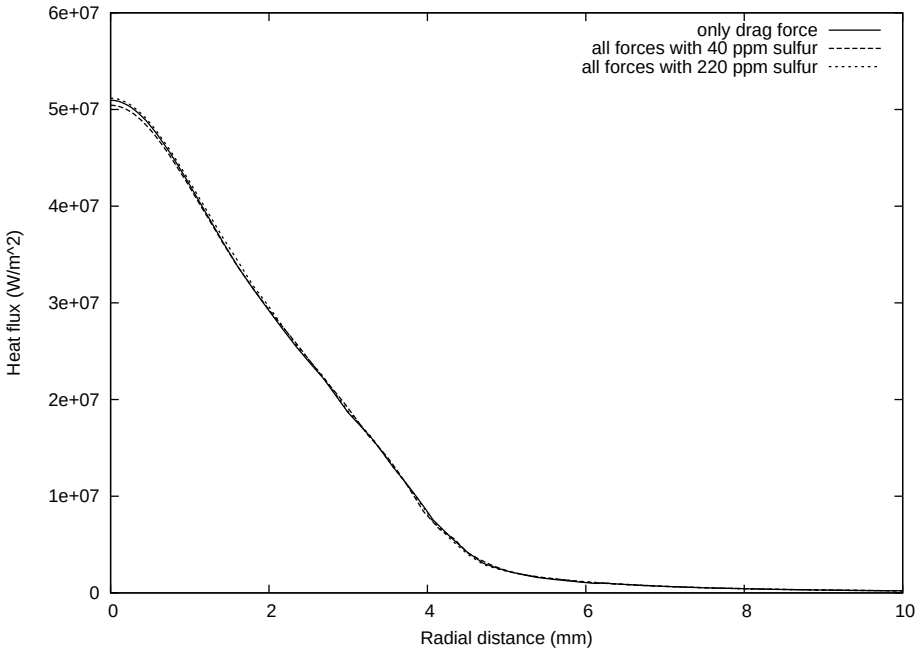

Heat flux ($W \cdot m^{-2}$) on the anode surface for different weld pool shapes

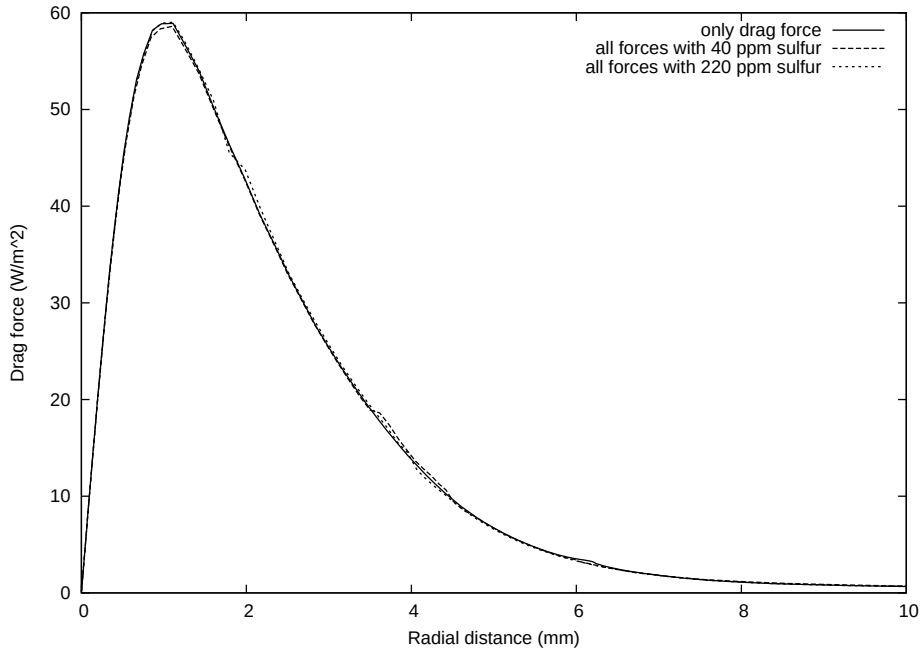

Arc drag force ($N \cdot m^{-2}$) on the anode surface for different weld pool shapes

- For this configuration, no influence of the weld pool shapes on the arc drag forces and the heat flux transferred to the workpiece
  $\longrightarrow$ after solving the whole problem, arc drag force and heat flux can be applied as boundary conditions of a weld pool model

Conclusions

- A model including arc and weld pool physics with dependance on the sulfur activity has been developped.
- Results give a good accordance with experimantal results.
- The predominant forces are the arc drag force and the force due to surface tension gradient that depends on the sulfur concentration.
- Heat flux and arc drag force obtained from a complete model can be used for solving a reduced weld pool model.

References

P. Fauchais.

Thermal Plasmas : fundamentals and applications, vol. 1.
1994.

B. Jiang.

The Least Square Finite Element Method.
1998.

C.S. Kim.

Thermophysical properties of stainless steels.
Master's thesis, Argonne national laboratory, 1975.

J.J. Lowke and M. Tanaka.

'lte diffusion approximation' for arc calculations.
Journal of Physics D : Applied Physics, 39 :3634–3643, 2006.

P. Sahoo, T. Debroy, and M. McNallan.

Surface tension of binary metal - surface active solute systems under conditions relevant to welding metallurgy.
Metallurgical and Materials Transactions B, 19 :483–491, 1988.

M. Tanaka and J.J. Lowke.

Predictions of weld pool profiles using plasma physics.
Journal of Physics D : Applied Physics, 40(1) :R1–R23, 2007.